



BN Tetracene: Extending the Reach of BN/CC Isosterism in Acenes

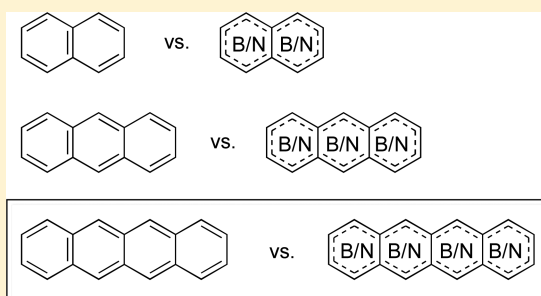
Jacob S. A. Ishibashi,[†] Alain Dargelos,[‡] Clovis Darrigan,[‡] Anna Chrostowska,^{*,‡} and Shih-Yuan Liu^{*,†}

[†]Department of Chemistry, Merkert Chemistry Center, Boston College, Chestnut Hill, Massachusetts 02467-3860, United States

[‡]Institut des Sciences Analytiques et de Physico-Chimie pour l'Environnement et les Matériaux, UMR CNRS 5254, Université de Pau et des Pays de l'Adour, Avenue de l'Université, 64 000 Pau, France

Supporting Information

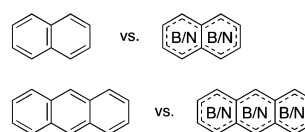
ABSTRACT: The first synthesis of a tetracene BN isostere is reported. Comparison with its direct, all-carbon analogue reveals that the BN tetracene isostere exhibits a lower-lying HOMO and a slightly larger optical HOMO–LUMO gap. While all-carbon tetracenes are prone to photodecomposition, the BN tetracene scaffold is less light sensitive, owing in part to its much higher photoluminescence quantum yield. In the context of this larger BN tetracene family, we introduce simple guiding principles for predicting frontier orbital energies as a function of the position of the BN unit within the tetracene scaffold.



Acenes, or polycyclic aromatic hydrocarbons (PAHs) featuring linearly fused benzene rings,¹ have demonstrated potential utility in organic-based optoelectronic devices.² For example, single-crystalline rubrene, a tetraphenyl-substituted tetracene, is considered a benchmark hole carrier, with a charge mobility of up to 40 cm² V⁻¹ s⁻¹.³ Similarly, pentacene derivatives have exhibited useful field-effect mobility in organic thin-film transistors.⁴ The success of acenes in materials research has spurred the development of heteroacenes to achieve electronic structure perturbations to complement carbonaceous acenes.⁵ We and others have been pursuing the BN/CC isosterism approach,⁶ i.e., the replacement of a CC unit with an isoelectronic BN unit, as a way to diversify the chemical space of linearly fused benzene rings.⁷ Previously, we reported the synthesis of BN naphthalenes⁸ and BN anthracenes⁹ and described the consequences of BN/CC isosterism on the electronic structure of these “lower” acenes. However, if BN/CC isosterism is to be exploited for further optoelectronic materials research, the synthesis and investigation of BN isosteres of higher acenes (tetracene, pentacene, hexacene, etc.) would be necessary. To the best of our knowledge, the preparation and electronic structure analysis of BN tetracene¹⁰ or its higher acene derivatives have not been reported. In this communication, we describe the first synthesis of a BN tetracene derivative. Its electronic structure analysis via UV–vis absorption/emission spectroscopy, electrochemistry, and quantum chemical calculation in direct comparison to its carbonaceous counterpart reveals that the BN tetracene analogue has a lower HOMO energy level, a larger optical HOMO–LUMO gap, and a significantly higher photoluminescence quantum yield in comparison to the corresponding all-carbon tetracene. Furthermore, we use the tetracene framework to introduce a new frontier orbital analysis that now can predict whether the frontier orbitals (HOMO and LUMO) of a BN acene isomer will be raised or lowered relative to its

carbonaceous counterpart simply on the basis of the structure of the HOMO/LUMO of the reference carbonaceous acene in question and the positioning of the BN unit (Figure 1).

previous work:



this work:

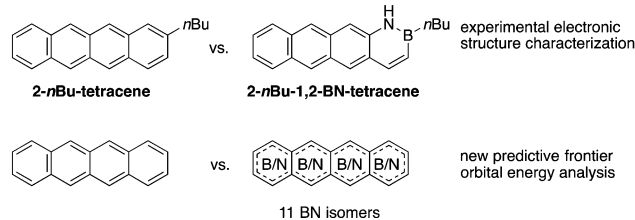


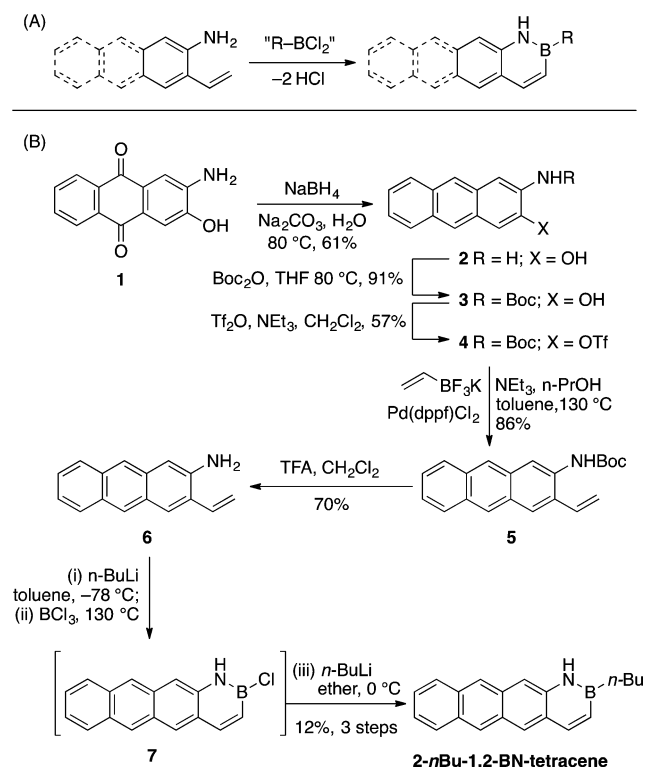
Figure 1. Synthesis and comparative electronic structure characterization of BN tetracenes.

We initially sought to adapt Dewar’s original aromatic borylation approach (Scheme 1A),¹¹ which condenses 2-vinyl arylamines with R-BCl₂ species to furnish the BN acene target.¹² We and Klausen have previously used this strategy for the construction of the heterocyclic portion of BN anthracenes.^{9,13} Thus, we synthesized cyclization precursor 2-amino-3-vinylanthracene (6) using the sequence illustrated in

Special Issue: Tailoring the Optoelectronic Properties of Organometallic Compounds with Main Group Elements

Received: April 17, 2017

Published: May 24, 2017

Scheme 1. Synthesis of 2-*n*Bu-1,2-BN-tetracene

Scheme 1B.¹⁴ Unfortunately, heating **6** to reflux in toluene with boron trichloride or phenylboron dichloride, conditions identical with those used in the syntheses of BN anthracene and BN naphthalene, returned only starting precursor **6**. We also attempted Molander's halogen exchange reactions of potassium alkyl- and aryltrifluoroborate salts to no avail.^{12b} We hypothesized that the extended conjugation in **6** may have rendered the nitrogen lone pair less nucleophilic toward the necessary coordination to the boron atom.¹⁵ To overcome this challenge, we first treated the cyclization precursor **6** with *n*-butyllithium followed by the addition of boron trichloride.^{7h} Heating the resulting mixture to reflux produced B-Cl BN tetracene **7**, which we did not isolate. Rather, direct treatment of the crude boron chloride **7** with *n*-butyllithium gave 2-*n*Bu-1,2-BN-tetracene as a yellow solid. Though the butyl group lends more solubility to the molecule than would be expected from the parent BN tetracene, 2-*n*Bu-1,2-BN-tetracene remains only sparingly soluble in most common organic solvents; this poor solubility prevented us from growing single crystals suitable for X-ray analysis.¹⁶

Figure 2 shows the UV-vis spectra of 2-*n*Bu-1,2-BN-tetracene and its carbonaceous analogue 2-*n*Bu-tetracene¹⁷ along with a table summarizing key parameters associated with their optoelectronic properties. The lowest-energy absorption peak for 2-*n*Bu-tetracene is at 446 nm, while the corresponding peak for 2-*n*Bu-1,2-BN-tetracene can be found at 427 nm. According to TD-DFT calculations, this transition can be ascribed to the $S_0 \rightarrow S_1$ transition that involves a HOMO \rightarrow LUMO excitation. **Figure 2** also shows a second electronic transition peak in the 330–500 nm window for 2-*n*Bu-1,2-BN-tetracene that is located at 380 nm. This higher-energy band is predicted by TD-DFT to have a relatively stronger oscillator strength and originates from the transition of HOMO-1 \rightarrow LUMO with some additional involvement of the HOMO to

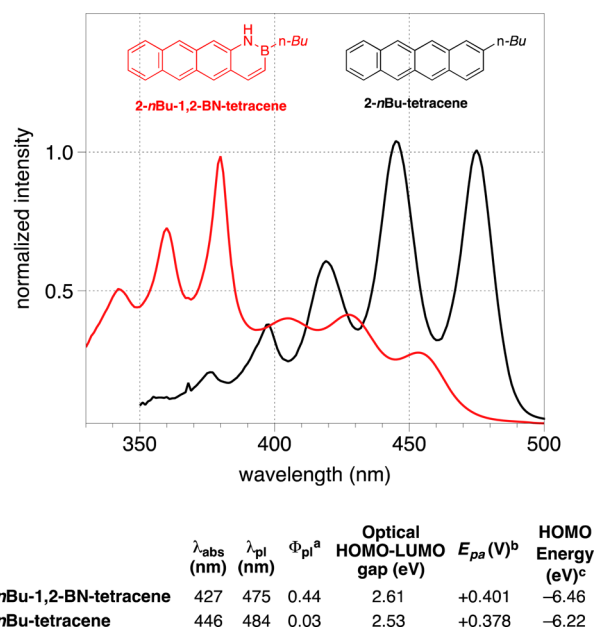


Figure 2. Normalized absorption spectra taken in methylene chloride solvent. Legend: (a) quantum yield measured using an integrating sphere; (b) anodic peak potentials (E_{pa}) measured by cyclic voltammetry (0.1 M $\text{Bu}_4\text{NBF}_4/\text{DMF}$, V vs the ferrocene/ferrocenium redox couple); (c) calculated at the CAM-B3LYP/6-311G(d,p) level.

LUMO+1 and LUMO+2 transitions. On the other hand, the transition to the second excited state for the carbonaceous 2-*n*Bu-tetracene is predicted to have a significantly higher energy with a relatively low oscillator strength, consistent with experimental observations.¹⁸

In contrast to our observations with the BN anthracene series, which shows a slightly smaller optical HOMO–LUMO gap for the 1,2-BN-anthracene isostere (3.22 eV) vs anthracene (3.26 eV),⁹ the experimentally determined optical HOMO–LUMO gap¹⁹ for 2-*n*Bu-1,2-BN-tetracene (2.61 eV) is actually slightly larger than that for 2-*n*Bu-tetracene (2.53 eV). A second distinguishing observation pertains to the photoluminescence quantum yield. In the anthracene series the photoluminescence quantum yield for anthracene ($\Phi_{\text{pl}} = 0.36$) is very similar to that for 1,2-BN-anthracene ($\Phi_{\text{pl}} = 0.38$).⁹ For this tetracene series, the photoluminescence quantum yield determined for 2-*n*Bu-1,2-BN-tetracene ($\Phi_{\text{pl}} = 0.44$) is significantly larger than that observed for the carbonaceous 2-*n*Bu-tetracene ($\Phi_{\text{pl}} = 0.03$).²⁰

On the basis of the observed differences in photoluminescence quantum yield, it is tempting to hypothesize that the all-carbon 2-*n*Bu-tetracene may be more prone to engage in nonradiative photochemistry pathways. Indeed, more than 50% of 2-*n*Bu-tetracene degraded over 4 h in degassed methylene chloride solution (ca. 3.3×10^{-5} M) under ambient light from a fluorescent lamp, as measured by the disappearance of the absorption band at 446 nm.²¹ In contrast, 2-*n*Bu-1,2-BN-tetracene does not photobleach in solution (5.64×10^{-4} M) over 4 h under the same light exposure.

We used electrochemistry to evaluate the relative HOMO energy levels of the tetracene derivatives. 2-*n*Bu-1,2-BN-tetracene undergoes an irreversible oxidation at the anodic peak potential $E_{\text{pa}} = +0.401$ V vs the ferrocene/ferrocenium couple in *N,N*-dimethylformamide/0.1 M Bu_4NBF_4 (see the **Supporting Information**). On the other hand, 2-*n*Bu-tetracene

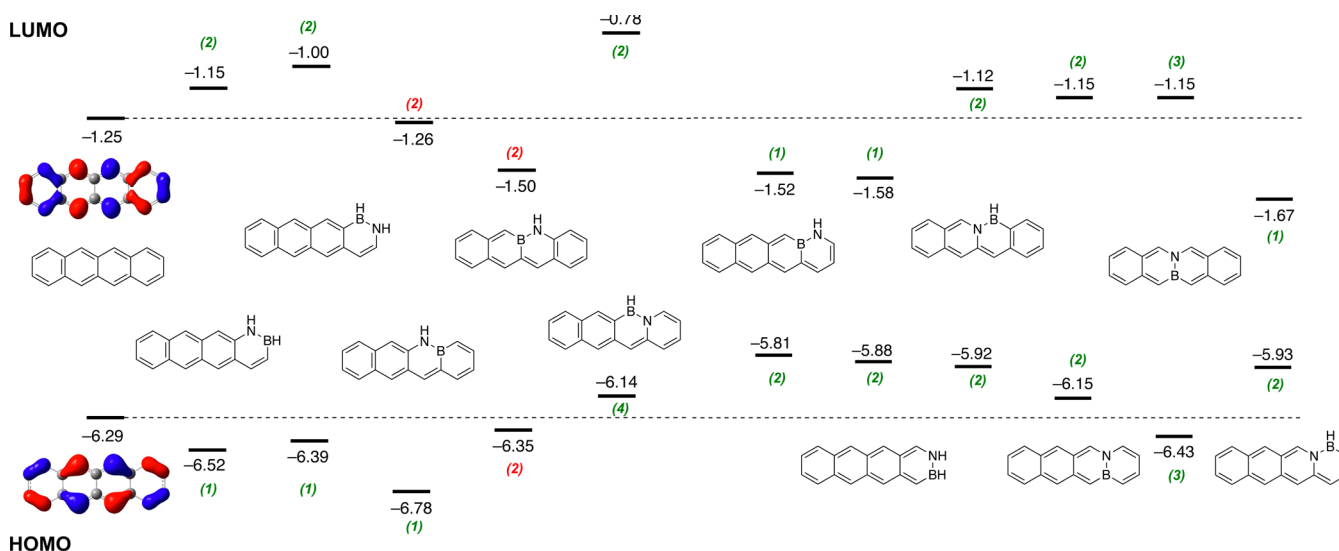


Figure 3. Application of the empirical frontier orbital energy correlation to the BN tetracene series. Orbital energies are given in eV, calculated at the CAM-B3LYP/6-311G(d,p) level.

irreversibly oxidizes at an E_{pa} value of +0.378 V, which is at a potential lower than that observed for 2-*n*Bu-1,2-BN-tetracene. The electrochemical data are consistent with DFT calculations that predict a lower-lying HOMO for 2-*n*Bu-1,2-BN-tetracene in comparison to its all-carbon analogue (table in Figure 2).

There are in total 11 BN tetracene isomers. Depending on the positioning of the BN unit, the frontier orbitals and consequently the electronic structure of these BN heterocycles can vary quite dramatically (Figure 3). In the context of these BN tetracene isomers, we introduce here a simple empirical model that can predict (with exceptions) whether the frontier orbitals (HOMO or LUMO) of a given BN isomer are stabilized or destabilized vs the corresponding frontier orbitals of the all-carbon tetracene on the basis of the electronic structure of the frontier orbital of the carbonaceous system and the positioning of the BN unit. In developing our empirical model, we evaluated the electronic structures of the naphthalene, anthracene, and tetracene series and arrived at the following principles.

(1) If the BN bond is located in the acene scaffold where the all-carbon analogue's frontier orbital (HOMO or LUMO) contains a bonding interaction (same phase) and where the N atom occupies a position with the larger orbital coefficient, then the frontier orbital (HOMO or LUMO) will be stabilized vs that of the all-carbon analogue.

(2) If the BN bond is located where the all-carbon analogue's frontier orbital (HOMO or LUMO) shows an antibonding (opposite phase) or a nonbonding interaction, then the frontier orbital (HOMO or LUMO) will be destabilized vs that of the all-carbon analogue.

(3) If the BN bond is located at a node, then the HOMO of the BN isostere will be stabilized and the LUMO of the BN isostere will be destabilized vs that of the all-carbon analogue.

(4) If the BN bond is located at a bonding region with respect to the all-carbon analogue's HOMO but the nitrogen atom occupies a position with a relatively smaller orbital coefficient, then the HOMO energy of the BN isostere will be destabilized vs that of the all-carbon analogue.

Figure 3 shows the application of this empirical analysis to the 11 BN tetracene isomers. The applied empirical principle is given in parentheses. A green color coding indicates that the

orbital energies obtained from DFT calculations are consistent with our empirical model. A red color coding indicates outliers. As can be seen from Figure 3 and from our analysis of the naphthalene and anthracene series (i.e., a total of 50 frontier orbitals; see the Supporting Information for the complete set), six exceptions to our principles are observed (5 of them associated with virtual orbitals). Thus, the presented predictive frontier orbital energy model will allow the synthetic chemist to quickly estimate the frontier orbital energies (including the HOMO–LUMO gap) of the BN isostere relative to the all-carbon reference simply from its Lewis structure.

In summary, we have successfully synthesized the first example of a BN tetracene analogue. Its electronic structure characterizations revealed that the BN tetracene analogue has a lower HOMO energy level, a larger optical HOMO–LUMO gap, and a significantly higher photoluminescence quantum yield in comparison to the corresponding all-carbon tetracene. We also provided in the context of the BN tetracene series a set of empirical guiding principles that allows the prediction of frontier orbital energetics based on the positioning of the BN unit and the knowledge of the electronic structure of the carbonaceous reference. These empirical principles should be generally applicable to acene scaffolds, including higher acenes, and thus should be useful in the further targeted syntheses of BN acenes for optoelectronic applications.

■ ASSOCIATED CONTENT

Supporting Information

The Supporting Information is available free of charge on the ACS Publications website at DOI: 10.1021/acs.organo-
met.7b00296.

Experimental procedures, computational details, including the full reference for Gaussian 09, supplemental photophysical studies, cyclic voltammograms, and NMR spectra for new compounds (PDF)

Cartesian coordinates of computed compounds (XYZ)

■ AUTHOR INFORMATION

Corresponding Authors

*E-mail for A.C.: anna.chrostowska@univ.pau.fr.

*E-mail for S.-Y.L.: shihyuan.liu@bc.edu.

ORCID

Shih-Yuan Liu: 0000-0003-3148-9147

Notes

The authors declare no competing financial interest.

ACKNOWLEDGMENTS

This research was supported by the National Science Foundation (CHE-1561153). We acknowledge Dr. Jonathan L. Marshall for scouting potential synthetic routes. We also thank Dr. Audrey Mazière for preliminary computational work. J.S.A.I. thanks the LaMattina Family Fellowship in Chemical Synthesis for support.

REFERENCES

- (1) Harvey, R. G. *Polycyclic Aromatic Hydrocarbons*; Wiley-VCH: Chicago, 1997.
- (2) (a) Anthony, J. E. *Angew. Chem., Int. Ed.* **2008**, *47*, 452–483. (b) Wang, C.; Dong, H.; Hu, W.; Liu, Y.; Zhu, D. *Chem. Rev.* **2012**, *112*, 2208–2267. (c) Dong, H.; Fu, X.; Liu, J.; Wang, Z.; Hu, W. *Adv. Mater.* **2013**, *25*, 6158–6183.
- (3) Hasegawa, T.; Takeya. *Sci. Technol. Adv. Mater.* **2009**, *10*, 024314.
- (4) Sheraw, D.; Jackson, N.; Eaton, L.; Anthony, E. *Adv. Mater.* **2003**, *15*, 2009–2011.
- (5) For an overview see: (a) Anthony, J. E. *Chem. Rev.* **2006**, *106*, 5028–5048. (b) Bunz, U. H. F.; Engelhart, J. U.; Lindner, B. D.; Schaffroth, M. *Angew. Chem., Int. Ed.* **2013**, *52*, 3810–3821. (c) Lorbach, A.; Hübner, A.; Wagner, M. *Dalton Trans.* **2012**, *41*, 6048–6063. For examples of recent N-doped acenes, see: (d) Lehnher, D.; Alzola, J. M.; Mulzer, C. R.; Hein, S. J.; Dichtel, W. R. *J. Org. Chem.* **2017**, *82*, 2004–2010. (e) Lindner, B. D.; Engelhart, J. U.; Tverskoy, O.; Appleton, A. L.; Rominger, F.; Peters, A.; Himmel, H.-J.; Bunz, U. H. F. *Angew. Chem., Int. Ed.* **2011**, *50*, 8588–8591. (f) Engelhart, J. U.; Lindner, B. D.; Tverskoy, O.; Rominger, F.; Bunz, U. H. F. *Chem. - Eur. J.* **2013**, *19*, 15089–15092. For recent examples of B-doped acenes, see: (g) Chen, J.; Kampf, J. W.; Ashe, A. J. *Organometallics* **2008**, *27*, 3639–3641. (h) Hoffend, C.; Schödel, F.; Bolte, M.; Lerner, H. W.; Wagner, M. *Chem. - Eur. J.* **2012**, *18*, 15394–15405. (i) John, A.; Bolte, M.; Lerner, H.; Wagner, M. *Angew. Chem., Int. Ed.* **2017**, *56*, 5588–5592.
- (6) For an overview, see: (a) Liu, Z.; Marder, T. B. *Angew. Chem., Int. Ed.* **2008**, *47*, 242–244. (b) Bosdet, M. J. D.; Piers, W. E. *Can. J. Chem.* **2009**, *87*, 8–29. (c) Campbell, P. G.; Marwitz, A. J. V.; Liu, S.-Y. *Angew. Chem., Int. Ed.* **2012**, *51*, 6074–6092. (d) Morgan, M. M.; Piers, W. E. *Dalton Trans.* **2016**, *45*, 5920–5924.
- (7) For select examples of BN isosteres of polycyclic aromatic hydrocarbons, see: (a) Yang, D.-T.; Møllerup, S. K.; Peng, J.-B.; Wang, X.; Li, Q. S.; Wang, S. J. *Am. Chem. Soc.* **2016**, *138*, 11513–11516. (b) Davies, G. H. M.; Zhou, Z.-Z.; Jouffroy, M.; Molander, G. A. J. *Org. Chem.* **2017**, *82*, 549–555. (c) Ma, C.; Zhang, J.; Li, J.; Cui, C. *Chem. Commun.* **2015**, *51*, 5732–5734. (d) Morgan, M. M.; Patrick, E. A.; Rautiainen, J. M.; Tuononen, H. M.; Piers, W. E.; Spasyuk, D. M. *Organometallics* **2017**, DOI: 10.1021/acs.organomet.7b00051. (e) Rohr, A. D.; Kampf, J. W.; Ashe, A. J., III *Organometallics* **2014**, *33*, 1318–1321. (f) Wang, X.-Y.; Lin, H.-R.; Lei, T.; Yang, D.-C.; Zhuang, F.-D.; Wang, J. Y.; Yuan, S.-C.; Pei, J. *Angew. Chem., Int. Ed.* **2013**, *52*, 3117–3120. (g) Zhuang, F.-D.; Han, J.-M.; Tang, S.; Yang, J.-H.; Chen, Q.-R.; Wang, J.-Y.; Pei, J. *Organometallics* **2017**, DOI: 10.1021/acs.organomet.6b00811. (h) Hatakeyama, T.; Hashimoto, S.; Seki, S.; Nakamura, M. *J. Am. Chem. Soc.* **2011**, *133*, 18614–18617. (i) Hashimoto, S.; Ikuta, T.; Shiren, K.; Nakatsuka, S.; Ni, J.; Nakamura, M.; Hatakeyama, T. *Chem. Mater.* **2014**, *26*, 6265–6271. (j) Wang, X.; Zhang, F.; Liu, J.; Tang, R.; Fu, Y.; Wu, D.; Xu, Q.; Zhuang, X.; He, G.; Feng, X. *Org. Lett.* **2013**, *15*, 5714–5717. (k) Zhang, W.; Zhang, F.; Tang, R.; Fu, Y.; Wang, X.; Zhuang, X.; He, G.; Feng, X. *Org. Lett.* **2016**, *18*, 3618–3621. (l) Wang, S.; Yang, D. T.; Lu, J.; Shimogawa, H.; Gong, S.; Wang, X.; Møllerup, S. K.; Wakamiya, A.; Chang, Y. L.; Yang, C.; Lu, Z. H. *Angew. Chem., Int. Ed.* **2015**, *54*, 15074–15078.
- (8) (a) Brown, A. N.; Li, B.; Liu, S.-Y. *J. Am. Chem. Soc.* **2015**, *137*, 8932–8935. (b) Liu, Z.; Ishibashi, J. S. A.; Darrigan, C.; Dargelos, A.; Chrostowska, A.; Li, B.; Vasiliu, M.; Dixon, D. A.; Liu, S.-Y. *J. Am. Chem. Soc.* **2017**, *139*, 6082–6085.
- (9) Ishibashi, J. S. A.; Marshall, J. L.; Mazière, A.; Lovinger, G. J.; Li, B.; Zakharov, L. N.; Dargelos, A.; Gracia, A.; Chrostowska, A.; Liu, S.-Y. *J. Am. Chem. Soc.* **2014**, *136*, 15414–15421.
- (10) We define BN tetracene or higher BN acene derivatives as the corresponding linearly fused polycyclic aromatic hydrocarbon in which a connected C=C bond unit has been directly replaced with a BN bond unit. For a computational study of BN tetracenes, see: Ghosh, D.; Periyasamy, G.; Pati, S. K. *Phys. Chem. Chem. Phys.* **2011**, *13*, 20627–20636.
- (11) Dewar, M. J. S.; Dietz, R. J. *Chem. Soc.* **1959**, 2728–2730.
- (12) (a) Paetzold, P.; Stanesco, C.; Stubenrauch, J. R.; Bienmueller, M.; Englert, U. Z. *Anorg. Allg. Chem.* **2004**, *630*, 2632–2640. (b) Wisniewski, S. R.; Guenther, C. L.; Argintaru, O. A.; Molander, G. A. *J. Org. Chem.* **2014**, *79*, 365–378. (c) Molander, G. A.; Wisniewski, S. R.; Amani, J. *Org. Lett.* **2014**, *16*, 5636–5639. (d) Molander, G. A.; Wisniewski, S. R. *J. Org. Chem.* **2014**, *79*, 6663–6678.
- (13) van de Wouw, H. L.; Lee, J. Y.; Siegler, M. A.; Klausen, R. S. *Org. Biomol. Chem.* **2016**, *14*, 3256–3263.
- (14) Synthetic steps adapted from: (a) Dadvand, A.; Moiseev, A. G.; Sawabe, K.; Sun, W.-H.; Djukic, B.; Chung, I.; Takenobu, T.; Rosei, F.; Perepichka, D. F. *Angew. Chem., Int. Ed.* **2012**, *51*, 3837–3841. (b) Li, G.-Q.; Gao, H.; Keene, C.; Devonas, M.; Ess, D. H.; Kürti, L. *J. Am. Chem. Soc.* **2013**, *135*, 7414–7417.
- (15) See the [Supporting Information](#) for a comparison between the HOMOs of compound **6** and 3-vinylnaphthalen-2-amine.
- (16) We attempted to synthesize the parent compound by treating crude **7** with lithium aluminum hydride. However, this reaction gave an intractable mixture, in contrast to a similar reaction in the syntheses of parent BN-1,2-naphthalene and BN-1,2-anthracene. We also attempted B-aryl substitution, but the reactions of aryllithium and aryl Grignard reagents with the crude **7** resulted in complex mixtures.
- (17) For the synthesis of 2-nBu-tetracene, see the [Supporting Information](#): (a) Li, H.; Zhong, Y. L.; Chen, C. Y.; Ferraro, A. E.; Wang, D. *Org. Lett.* **2015**, *17*, 3616–3619. (b) Shu, Y.; Lim, Y.-F.; Li, Z.; Purushothaman, B.; Hallani, R.; Kim, J. E.; Parkin, S. R.; Malliaras, G. G.; Anthony, J. E. *Chem. Sci.* **2011**, *2*, 363–368. (d) Kitamura, C.; Ohe, G.; Kawase, T.; Saeki, A.; Seki, S. *Bull. Chem. Soc. Jpn.* **2014**, *87*, 915–921.
- (18) See the [Supporting Information](#) for the TD-DFT calculations and the full UV–vis spectra of 2-nBu-tetracene and 2-nBu-1,2-BN-tetracene.
- (19) The optical HOMO–LUMO gap has been determined using the intersection of the *x* axis by the line tangent to the onset of the lowest-energy absorption peak.
- (20) Relatively low quantum yields are expected from tetracene and alkyltetracenes in solution; see: Kitamura, C. *Chem. Rec.* **2012**, *12*, 506–514.
- (21) This degradation likely corresponds to tetracene dimer formation; see: Lapouyade, R.; Nourmamide, A.; Bouaslaurent, H. *Tetrahedron* **1980**, *36*, 2311–2316.